



**HAL**  
open science

## Optimization of organized silicon nanowires growth inside porous anodic alumina template using hot wire chemical vapor deposition process

E. Lefeuvre, K.H. Kim, J.-L. Maurice, Marc Châtelet, D. Pribat, C.S. Cojocaru

### ► To cite this version:

E. Lefeuvre, K.H. Kim, J.-L. Maurice, Marc Châtelet, D. Pribat, et al.. Optimization of organized silicon nanowires growth inside porous anodic alumina template using hot wire chemical vapor deposition process. *Thin Solid Films*, 2011, 519, pp.4603. 10.1016/j.tsf.2011.01.333 . hal-00601287

**HAL Id: hal-00601287**

**<https://polytechnique.hal.science/hal-00601287>**

Submitted on 17 Jun 2011

**HAL** is a multi-disciplinary open access archive for the deposit and dissemination of scientific research documents, whether they are published or not. The documents may come from teaching and research institutions in France or abroad, or from public or private research centers.

L'archive ouverte pluridisciplinaire **HAL**, est destinée au dépôt et à la diffusion de documents scientifiques de niveau recherche, publiés ou non, émanant des établissements d'enseignement et de recherche français ou étrangers, des laboratoires publics ou privés.

# Optimization of organized silicon nanowires growth inside Porous Anodic Alumina template using Hot Wire Chemical Vapor Deposition process.

E. Lefeuvre<sup>1</sup>, K. H. Kim<sup>1</sup>, Z.B. He<sup>1</sup>, J-L Maurice<sup>1</sup>, M. Chatelet<sup>1</sup>, D. Pribat<sup>2</sup> and C.S. Cojocaru<sup>1</sup>

<sup>1</sup>Laboratoire de Physique des Interfaces et des Couches Minces, UMR 7647 CNRS/Ecole Polytechnique, PALAISEAU, France

<sup>2</sup>Departement of Energy Science, Sungkyunkwan University, Suwon, 440-746, Korea

Corresponding e-mail address: costel-sorin.cojocaru@polytechnique.edu

## Abstract

A Hot Wire assisted Chemical Vapor Deposition (HW-CVD) process has been developed for producing high-density arrays of parallel, straight and organized silicon nano-wires (SiNWs) inside vertical Porous Anodic Alumina (PAA) templates, exploring temperatures ranging from 430°C to 600°C, and pressures varying between 2.5 and 7.5 mbar. In order to prevent parasitic amorphous silicon (a-Si) deposit and to promote the crystalline SiNWs growth, we used a tungsten hot wire to partially crack H<sub>2</sub> into atomic hydrogen, which acts like a selective etchant regarding a-Si. Here we describe the optimization route we followed to limit the deposit of a-Si onto the surface of the porous membrane and on the walls of the pores, which led to the possibility to grow SiNWs inside the PAA membranes. Such approach has high potentialities for devices realization, like PIN junctions, FETs or electrodes for Li-ion batteries.

Keywords: hot wire CVD, silicon nanowires, porous alumina, PAA.

## 1. Introduction

Over the past years, an intense research activity has been devoted to the elaboration of 1D nanostructures, among which the silicon nanowires (SiNWs) are of high interest for developing future advanced electronic devices [1,2,3] or for integration in already-existing devices, because of their low cost and the wide-spread use of silicon in the microelectronics industry.

Most often, SiNWs synthesis is carried out by CVD methods based on the Vapor-Liquid-Solid (VLS) growth mechanism, first proposed by Wagner and Ellis in 1964 [4]. Such method, theoretically allows calibrating the length of the wires by varying the growth duration whilst the nanowire diameter can be controlled by the size of the catalyst droplet [5]. However some prerequisites are mandatory, such as obtaining a very narrow distribution of the size of the catalyst droplets (and maintaining it at the growth temperature) in order to get a good length/diameter uniformity of the grown NWs. A reliable and easy way to solve these problems is the use of templates to confine the growth of the nanostructures. In 1995, Masuda et al. developed a new process to obtain a very well-ordered porous structure, based on the anodization of an aluminium thin film [6]. Since then, such structure, usually called Porous Anodic Alumina (PAA) membrane, has been widely used in the field of nanowires/nanotubes growth because of its easily-controllable features, and the high aspect ratio of the pores [7,8,9,10,11]. Despite this progress, SiNWs growth still lacks a good control and understanding of the mechanisms that rule their formation [5,12,13,14], especially in such a very particular case where a confined growth occurs. This paper describes our work about SiNWs growth inside PAA templates using a HWCVD method.

## **2. Experimental section**

The PAA membranes were prepared by anodic oxidation of 1.2  $\mu\text{m}$ -thick aluminium layers on (100) silicon substrates. To provide a well-ordered PAA membrane, we performed a two-step anodization process as previously described [6]. The anodization process was carried out at 20V applied voltage with the sample as the anode and a graphite electrode as the cathode, in 0.3M sulfuric acid solutions cooled at 5°C. After the first anodization (about 3 min), the synthesized membrane was removed with a mixture of  $\text{CrO}_3$  and  $\text{H}_3\text{PO}_4$ , and the remaining aluminium layer was subsequently fully oxidized, yielding a 1.2 $\mu\text{m}$ -thick well-ordered porous alumina membrane with no pure Al left on the sample. The incorporation of oxygen ions and impurities (mainly coming from the acidic anodization solution) inside the Al layer leads to a volume expansion, i.e. a larger thickness of the final alumina layer than the initial aluminium layer. This is why the final PAA thickness reaches 1.2 $\mu\text{m}$ , even after removing the first-step anodization layer. We then used a 0.3M  $\text{H}_3\text{PO}_4$  solution at 30°C for 15 min in order to remove the possible residual alumina barrier layer at the bottom of some pores. After this process, the diameter of the pores is about  $30 \pm 5$  nm, with a mean inter-pore distance of about  $17 \pm 5$  nm.

The bottom of the pores of the as-prepared PAA membranes were seeded with copper catalyst nanoparticles (required for the SiNWs subsequent growth) by pulsed electrodeposition process using 1M solution of  $\text{CuSO}_4 \cdot 5\text{H}_2\text{O}$  ( $125 \text{ g}\cdot\text{L}^{-1}$ ) diluted in  $\text{H}_3\text{BO}_3$  ( $\approx 0.73\text{M}$ ,  $22.5 \text{ g}\cdot\text{L}^{-1}$ ). Electrodeposition of the catalyst was carried out with 5 ms pulses at -8.5V DC, for cations reduction at the bottom of the pores, each pulse being separated by a 90 ms rest time. This led to a partially-filled membrane (we estimated that more than 50% of the pores received a particle) with copper particles having a maximum length of 250 nm (insets of Fig 5a) and a diameter corresponding to the diameter of the pore.

SiNWs synthesis was carried out in a homemade Hot-Wire assisted CVD system at temperatures ranging from 430°C to 600°C, controlled by heating elements located outside

the quartz tube. The 0.5 mm diameter tungsten hot wire (ten-turn home-made spring) was powered from 0W to maximum 205W, corresponding to an approximate 1980°C temperature (optical pyrometer). Efficient H<sub>2</sub> decomposition is achieved by forcing its passage through the hot wire confined within a surrounding tantalum thermal screen placed on the internal wall of the furnace. The provided atomic hydrogen acts as an efficient etchant to remove undesired a-Si deposit on the surface or on the walls of the pores of the PAA membrane. Silane (SiH<sub>4</sub>), diluted in hydrogen was used as precursor gas for total pressures ranging from 2.5 to 7.5 mbar. Before starting the SiNWs growth (SiH<sub>4</sub> injection) the samples were exposed to atomic hydrogen for 5 minutes, in order to achieve clean and deoxidized catalyst surface.

### **3. Results and discussion**

#### *3.1. Growth process optimization*

An important challenge in the field of NWs growth is to prevent (or at least to limit) the formation of a parasitic amorphous phase of the deposited material. In the case of confined growth of SiNWs inside of PAA membranes we found a narrow window of suitable experimental conditions that avoid the excess deposit of a-Si: low pressure inside the reactor (in a few mbar range), relatively low growth temperature (<550°C) and low SiH<sub>4</sub>:H<sub>2</sub> ratio. In the following is described the optimization route we followed for optimizing the SiNWs growth conditions inside porous alumina membranes. For the sake of simplicity, only results that are useful for the understanding of our progression are reported.

When high pressure (7.5 mbar) and silane rate (SiH<sub>4</sub>:H<sub>2</sub> = 20:100 sccm) are employed, PAA surface is completely covered with amorphous silicon regardless of the

amount of atomic hydrogen generation. This is clearly illustrated in Fig 1a to Fig 1d where one can observe that even at high hot wire activation power (Fig 1d) the PAA surface is covered with a thick a-Si layer. In such extreme conditions, even at high-temperature-decomposed hydrogen, the amorphous silicon etching rate cannot overcome its high deposition rate. We can easily imagine that under such conditions silane molecules/radicals cannot diffuse to the catalyst particle located at the bottom of the pores.

Other conditions had to be found in order to avoid nanopores clogging, so that silane molecules could reach and decompose at the surface of the catalyst at the bottom of the pores. When only the gas ratio  $\text{SiH}_4:\text{H}_2$  is being decreased down to 10:100 sccm, while keeping a high hot wire activation power at 175W, etching conditions are not enough to prevent the formation of excess a-Si. To significantly decrease its deposition rate, it was necessary to simultaneously decrease both the total pressure and the  $\text{SiH}_4:\text{H}_2$  ratio inside the reactor. Fig 2 shows SEM observations of the samples on which growth have been performed at 4.0 mbar, 540°C, with a gas ratio of respectively  $\text{SiH}_4:\text{H}_2=5:95$  sccm (a) and  $\text{SiH}_4:\text{H}_2=2.5:97.5$  sccm (b). We chose to show a top view in this latter case in order to highlight the net improvement of the surface aspect of the porous membrane. Some big particles could still be observed on it, but overall the pores are still open at the PAA surface level even after a 30 minutes growth, which means that reactive gas molecules could now be able to access inside some pores and initiate SiNWs growth. Further optimization has been achieved by decreasing the overall pressure down to 2.5 mbar, while keeping all the other parameters unchanged, and the first evidences of intra-pore SiNWs growth clearly appeared (see Fig 3). Indeed, on one hand, some copper particles (appearing in brighter contrast) have clearly migrated upwards due to the SiNW growth, according to a Vapor-Solid-Solid (VSS) growth mechanism [15]. On the other hand, some materials

have formed underneath these particles (dashed circles), and appear in light gray, contrasting with dark black inside empty pores.

For the SiNWs catalyst assisted growth, silane decomposition rate has to be in the same range as the diffusion of Si atoms inside the solid alloy droplet [5, 16]. As SiH<sub>4</sub> decomposition rate is influenced by the growth temperature, it is reasonable to assume that an optimized growth temperature range has to be found for given process conditions. As we decreased the growth temperature from 540°C down to 490°C, we observed that PAA membranes were almost free of undesired-deposited a-Si, either on the surface or on the walls of the pores (Fig 4). The nanopores diameter at the PAA membrane surface level is also wider in this case, which confirms that the a-Si deposition rate has been dramatically reduced. Nevertheless, we weren't able to highlight any SiNWs growth in this case. Keeping in mind that the SiNWs growth rate is also strongly dependant on the growth temperature, this is probably due to too short process duration for such a low growth temperature. Indeed, given a size of a catalyst particle, and according to the VSS process (and even VLS), the catalyst particles have to get saturated by Si atoms (i.e Si has to reach its limit of solubility inside the catalyst-Si solid alloy) before solid Si could precipitate outside of the catalyst and thus form a wire [4,15]. Although a 30-minute growth time is relatively high compared to classical growth on free surfaces [13,14,17,18], it was probably not enough in our particular configuration, where due to confinement inside pores, there is only a very small exchange surface of the catalyst in regards to the precursor gas, which leads to increased incubation times. We thus extended the growth duration up to one hour while keeping a low total pressure of 2.5 mbar, the SiH<sub>4</sub>:H<sub>2</sub> ratio at 2.5:97.5 sccm, the power of filament at 175W and the temperature set-point at 490°C. As shown in Fig 5a, under such conditions, we can notice a visible intra-pore NWs growth, with reduced parasitic deposit on the walls of the pores. Like on Fig3, materials appearing in light gray

are topped by bright particles (Cu highlighted through backscattering electrons signal superposition on the secondary electron mode of the SEM). We performed a TEM analysis to support this result, and found some wires of several hundreds of nanometers in length, about 40 nm in diameter, with a twinned crystalline structure (Fig 5c). We may assume that this parameter window is suitable for a catalytic growth inside the pores, but also that a significantly longer incubation time is necessary to reach the Si saturation inside the catalyst droplet alloy for initiating the nanowires growth. We would also like to point out that when growth temperature range was enlarged to 430°C and 600°C respectively, no suitable result has been denoted (no NWs growth and too much a-Si deposit respectively).

### 3.2. *Influence of the hot wire*

As mentioned in the previous part, the amount of atomic hydrogen generation via the hot wire activation has little impact if the experimental conditions are too extreme (too high total pressure or gas ratio...) and favor high Si deposition rates. However, we can definitely see its influence upon the limitation of the deposit of amorphous silicon in a given window of conditions.

The following study continues the optimization of experimental conditions previously described ( $T_{\text{growth}} = 490^\circ\text{C}$ ,  $p = 2.5$  mbar,  $\text{SiH}_4:\text{H}_2 = 2.5:97.5$  sccm, 60 min), so as to determine the hot wire activation power starting from which atomic hydrogen generation become efficient in scavenging surplus a-Si deposition. As a starting point we performed an experiment keeping the hot wire off, i.e. the  $\text{H}_2$  been injected inside the furnace has no supplementary activation. The results are summarized in Fig 6. We can notice that the PAA nanopores walls appear to be covered with silicon (Fig 6a), which is clearly evidenced when comparing with the pre-growth sample (Fig 6c). The apparent diameter of the nanopores has decreased, indicating an accumulation of an amorphous phase onto the



substrate (Fig 6b). Such conditions are obviously not suitable for a proper NWs growth. We can compare these results with those showed in Fig 5, where growth had been performed with a hot wire activation power of 175W and in the same CVD conditions. We've already seen above that NWs growth was possible in these conditions while maintaining the PAA walls and surface rather clean, with little parasitic a-Si sparsely formed at some places of the sample. We thus performed another experiment, using an increased hot wire activation power of 205 W, corresponding to a wire temperature of about 1980°C (the other CVD parameter being constant). The results are shown in Fig 7 where we can notice a marked improvement, with a smoother aspect of the nanopores, almost identical to pre-growth aspect, proving the very good efficiency of atomic hydrogen as a scavenger for parasitic a-Si deposition. Nevertheless, it seems that the NWs growth rate has been also drastically decreased, as we couldn't evidence any growth on this sample.

In order to better evaluate the amount of silicon deposited on the nanopores walls, it appeared useful to remove the PAA membrane after the growth process. The membrane has been removed by an acidic etching, and we could recover intact Si nanowire-like structures, mostly formed from amorphous Si deposit and partly with crystalline structure. A study of the morphology and structure of the wires is described in [19]. Fig 8 shows samples corresponding to the three cases described above ( $P_f=0$ , 175 and 205W). We notice the presence of a large field of "bunches" of Si nano-objects when  $P_f=0$ W and  $P_f=175$ W (Fig 8a and 8b) after the removal of the alumina membrane, which shows that the amorphous Si layer deposited on the walls is thick enough to form solid straight structures, even with the filament on. In case of Fig 8b, we chose to show the "floating layer" made of amorphous silicon that remains on the top of the wires after the growth (due to amorphous Si deposition onto the surface of the membrane). In case of Fig 8a, this crust

had been removed using fluor-based Reactive Ion Etching prior to the membrane etching. On Fig 8c, which corresponds to the experiment with a hot wire activation power of 205W, we notice that such a crust is still present but that it's clearly closer to the substrate (about 130 nm from the surface of the substrate). This can be easily explained by the absence of amorphous silicon on the pore walls (as already mentioned, see Fig 7), that normally acts as supporting structure for the amorphous silicon crust after the membrane etching. If this silicon crust is etched prior to the membrane etching, we can reveal the surface of the substrate (Fig 8d). Its aspect is quite different from the previous samples ( $P_f=0W$  and  $P_f=175W$ ) as only some very sparse wires are visible on the surface, in contrast with the numerous dense wire bunches observed for the experiment at lower hot wire activation power. We may thus conclude that hydrogen activation via hot wire can be very efficient in preventing the formation of parasitic silicon structures, that couldn't be selectively removed from crystalline SiNWs after their growth. We could also find some vertical nano-structures that may be NWs. Further investigations are required to determine whether a high-density SiNWs growth is possible with such a high power.

#### **4. Conclusion**

SiNWs have been successfully grown inside PAA membrane, which is used as a template to collectively organize the NWs. A precise choice of experimental conditions is required in order to avoid parasitic silicon deposition that may clog the pores and thus prevent the NWs growth. An optimization of the CVD (total and partial pressure,  $SiH_4:H_2$  ratio, temperature) and the hot wire activation conditions has been performed, highlighting that when heated to temperatures higher than  $1900^{\circ}C$ , the hot wire efficiently generates atomic hydrogen for scavenging undesired Si deposition inside the nanopores.

## **Acknowledgment**

This work was partially funded by the NanodiX Chair with Samsung Electronics. The authors would like to thank Thales R&T, Palaiseau, for collaboration in NanoCarb research group.

## References

1. Cui, Y. & Lieber, C.M. Functional Nanoscale Electronic Devices Assembled Using Silicon Nanowire Building Blocks. *Science* **291**, 851-853 (2001).
2. Song, T. et al. Arrays of Sealed Silicon Nanotubes As Anodes for Lithium Ion Batteries. *Nano Lett.* **10**, 1710-1716 (2010).
3. Colinge, J. et al. Nanowire transistors without junctions. *Nature Nanotech* **5**, 225-229 (2010).
4. Wagner, R.S. & Ellis, W.C. VAPOR-LIQUID-SOLID MECHANISM OF SINGLE CRYSTAL GROWTH. *Appl. Phys. Lett.* **4**, 89 (1964).
5. Yao, Y. & Fan, S. Si nanowires synthesized with Cu catalyst. *Materials Letters* **61**, 177-181 (2007).
6. Masuda, H. & Fukuda, K. Ordered Metal Nanohole Arrays Made by a Two-Step Replication of Honeycomb Structures of Anodic Alumina. *Science* **268**, 1466-1468 (1995).
7. Mátéfi-Tempfli, S., Mátéfi-Tempfli, M., Vlad, A., Antohe, V. & Piraux, L. Nanowires and nanostructures fabrication using template methods: a step forward to real devices combining electrochemical synthesis with lithographic techniques. *Journal of Materials Science: Materials in Electronics* **20**, 249-254 (2009).
8. Bogart, T.E., Dey, S., Lew, K., Mohny, S. & Redwing, J. Diameter-Controlled Synthesis of Silicon Nanowires Using Nanoporous Alumina Membranes. *Advanced Materials* **17**, 114-117 (2005).
9. Xiang, Y. et al. Multiple Nanowire Species Synthesized on a Single Chip by Selectively Addressable Horizontal Nanochannels. *Nano Lett.* **10**, 1341-1346 (2010).
10. Byun, J., Lee, J.I., Kwon, S., Jeon, G. & Kim, J.K. Highly Ordered Nanoporous

- Alumina on Conducting Substrates with Adhesion Enhanced by Surface Modification: Universal Templates for Ultrahigh-Density Arrays of Nanorods. *Advanced Materials* **22**, 2028-2032 (2010).
11. Mu, C. et al. Uniform Metal Nanotube Arrays by Multistep Template Replication and Electrodeposition. *Advanced Materials* **16**, 1550-1553 (2004).
  12. Yan, X.Q. et al. H<sub>2</sub>-assisted control growth of Si nanowires. *Journal of Crystal Growth* **257**, 69-74 (2003).
  13. Mbenkum, B.N. et al. Low-Temperature Growth of Silicon Nanotubes and Nanowires on Amorphous Substrates. *ACS Nano* **4**, 1805-1812 (2010).
  14. Arbiol, J., Kalache, B., Cabarrocas, P.R.I., Morante, J.R. & Morral, A.F.I. Influence of Cu as a catalyst on the properties of silicon nanowires synthesized by the vapour–solid–solid mechanism. *Nanotechnology* **18**, 305606 (2007).
  15. Schmidt, V., Wittemann, J.V., Senz, S. & Gösele, U. Silicon Nanowires: A Review on Aspects of their Growth and their Electrical Properties. *Advanced Materials* **21**, 2681-2702 (2009).
  16. Lew, K. & Redwing, J.M. Growth characteristics of silicon nanowires synthesized by vapor-liquid-solid growth in nanoporous alumina templates. *Journal of Crystal Growth* **254**, 14-22 (2003).
  17. Qi, P., Wong, W.S., Zhao, H. & Wang, D. Low-temperature synthesis of Si nanowires using multizone chemical vapor deposition methods. *Appl. Phys. Lett.* **93**, 163101 (2008).
  18. Kikkawa, J., Ohno, Y. & Takeda, S. Growth rate of silicon nanowires. *Applied Physics Letters* (2005). [doi:10.1063/1.1888034](https://doi.org/10.1063/1.1888034)
  19. Lefeuvre, E. et al. Well organized Si nanowires arrays synthesis for electronic devices. 776105-776105-6 (2010). [doi:10.1117/12.863923](https://doi.org/10.1117/12.863923)

## List of figure captions

Fig 1. SEM cross sections of PAA after growth performed at 540°C, 7.5 mbar, SiH<sub>4</sub>:H<sub>2</sub> = 20:100 sccm for 30 min and hot wire power (P<sub>f</sub>): a) 0W, b) 150W, c) 175W and d) 205W.

Fig 2. PAA after growth performed at 540°C, 4.0 mbar, P<sub>f</sub> = 175W and SiH<sub>4</sub>:H<sub>2</sub> = a) 5:95 sccm (cross section) and b) 2:97.5 sccm (top view) for 30 min.

Fig 3. SEM cross section of a sample after growth performed at 540°C, 2.5 mbar, P<sub>f</sub> = 175W and SiH<sub>4</sub>:H<sub>2</sub> = 2.5:97.5 sccm

Fig 4. a) cross section and b) top view SEM pictures of a sample after growth performed at 490°C, 2.5 mbar, P<sub>f</sub> = 175W and SiH<sub>4</sub>:H<sub>2</sub> = 2:97.5 sccm.

Fig 5. a) cross section and b) top view of PAA after growth performed at 490°C, 2.5 mbar, P<sub>f</sub> = 175W and SiH<sub>4</sub>:H<sub>2</sub> = 2:97.5 sccm for 1h. c) TEM picture of a single twinned SiNW. The inset in a) corresponds to a sample before growth, showing the Cu particles (in bright).

Fig 6. SEM pictures of a sample a), b) after growth performed at 490°C, 2.5 mbar, P<sub>f</sub> = 0W and SiH<sub>4</sub>:H<sub>2</sub> = 2.5:97.5 sccm and c),d) before growth.

Fig 7. SEM cross sections of a sample after growth performed at 490°C, 2.5 mbar,  $P_f = 205\text{W}$  and  $\text{SiH}_4:\text{H}_2 = 2:97.5$  sccm.

Fig 8. SEM tilted views of a sample after growth and membrane removal, with a)  $P_f=0\text{W}$ , b)  $P_f=175\text{W}$ , c) and d)  $P_f=205\text{W}$ . In a) and d) the amorphous Si crust had been removed.

Fig 1

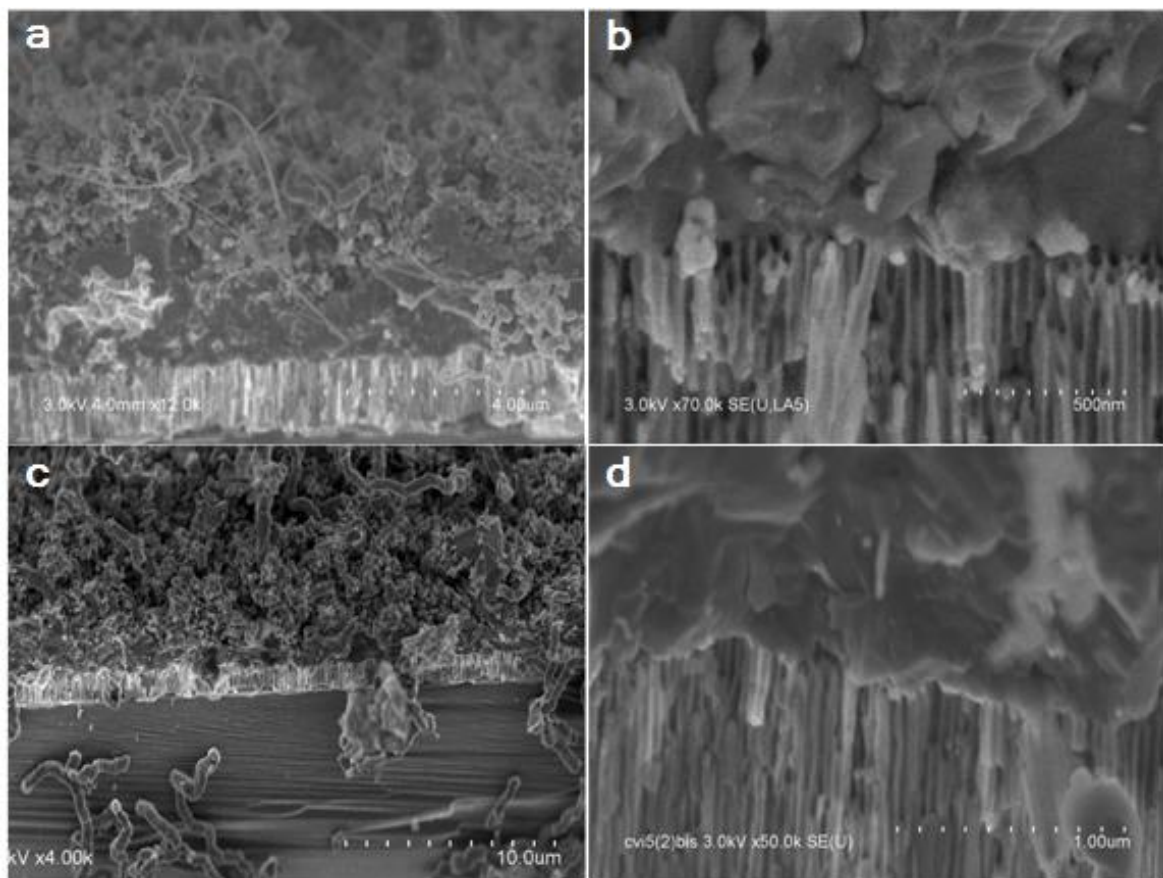




Fig 2

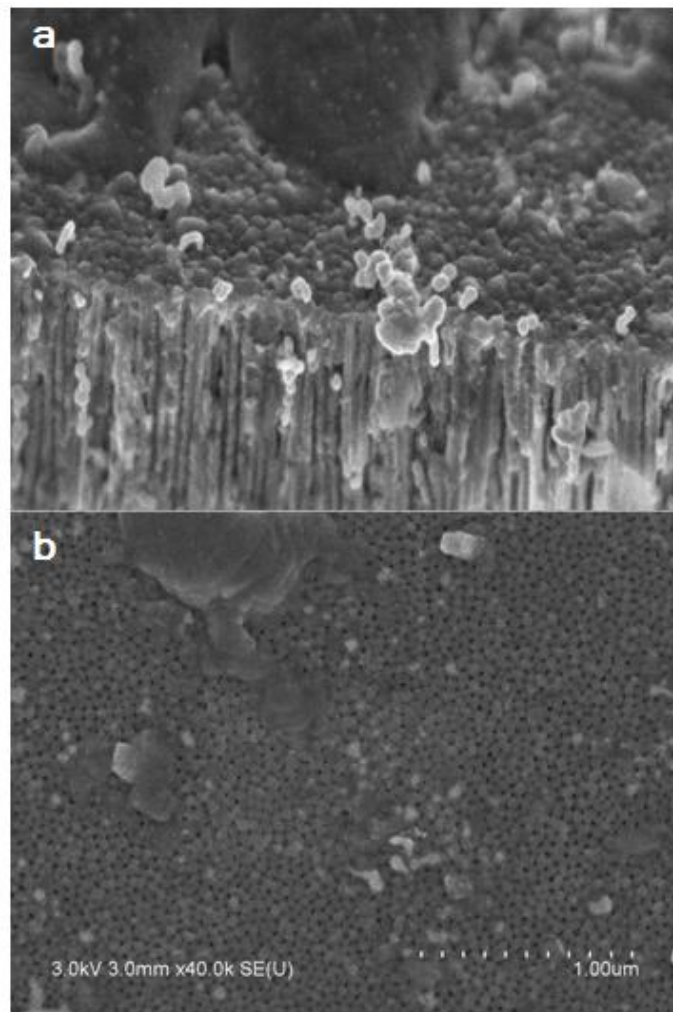


Fig 3

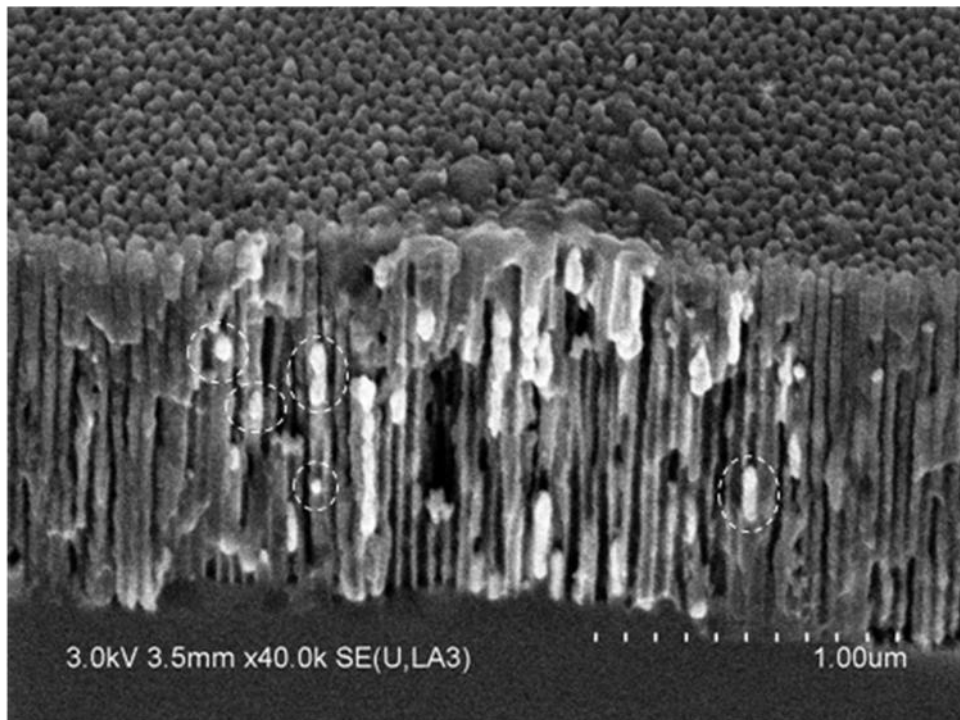


Fig 4

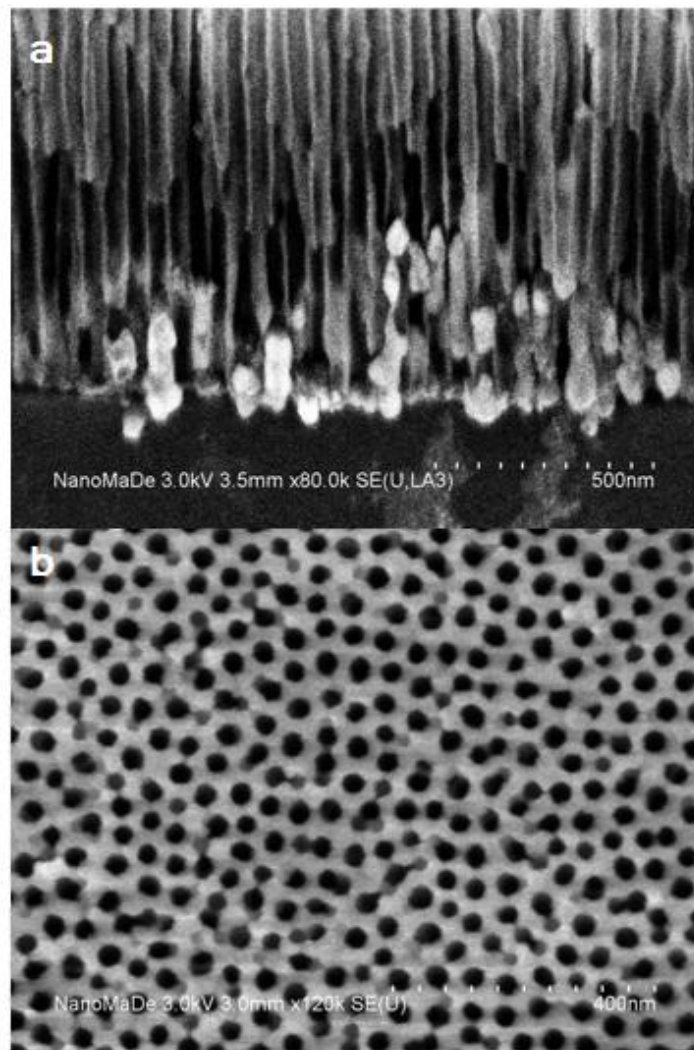


Fig 5

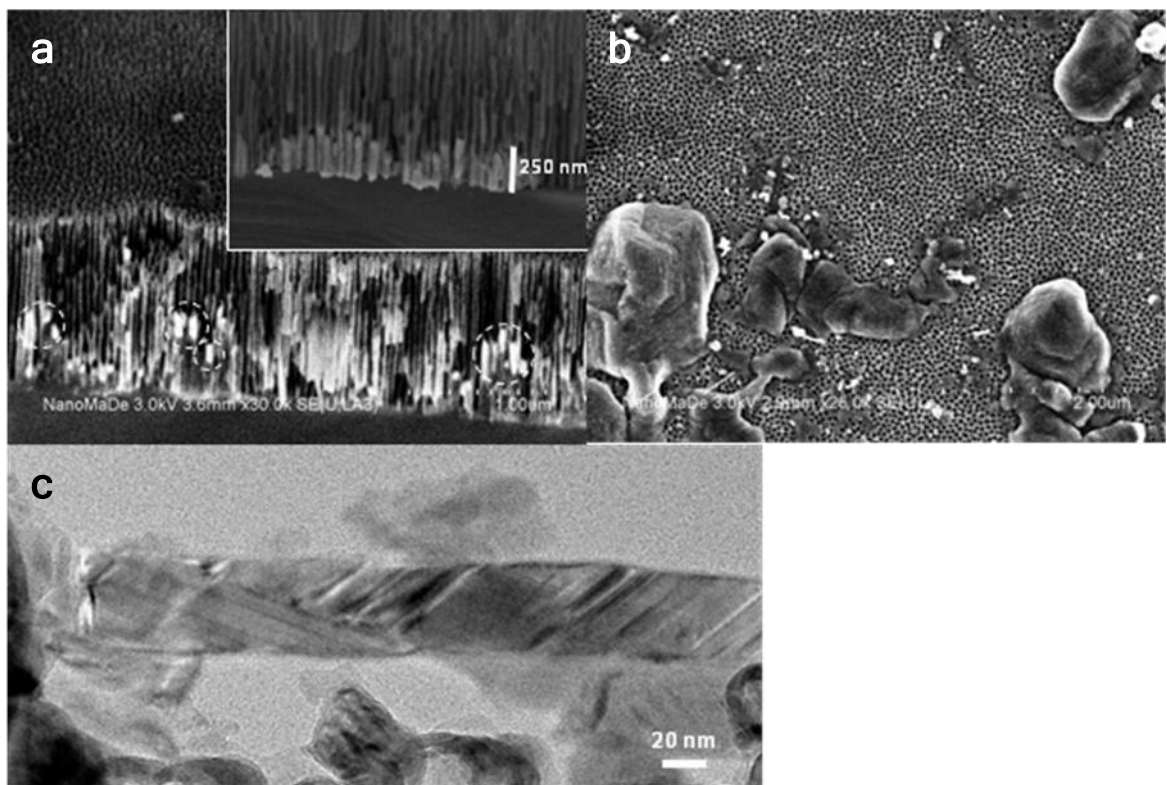


Fig 6

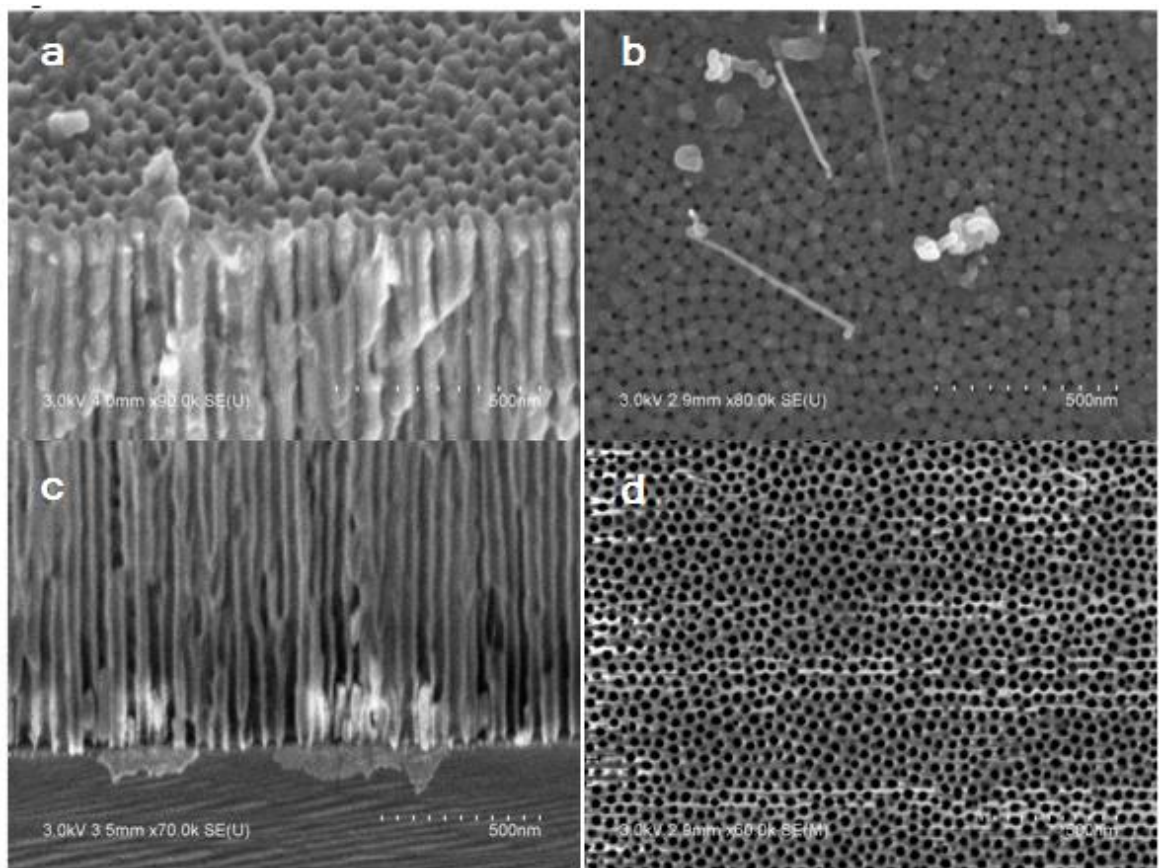


Fig 7

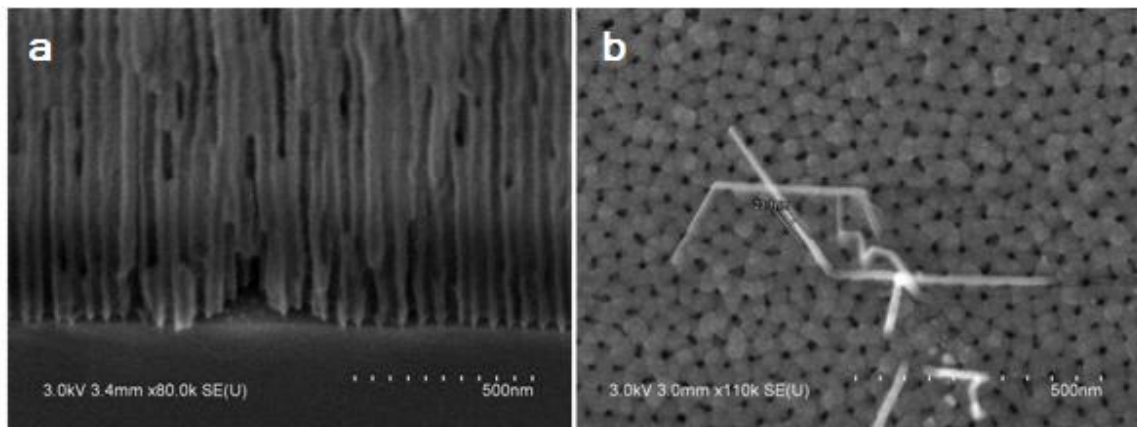


Fig 8

